Earth Syst. Dynam. Discuss., 6, 943–977, 2015
www.earth-syst-dynam-discuss.net/6/943/2015/
doi:10.5194/esdd-6-943-2015

Earth System Dynamics
Discussions
Open Access

Understanding land surface response to changing South Asian monsoon in a warming climate

M. V. S. Ramarao, R. Krishnan, J. Sanjay, and T. P. Sabin

Centre for Climate Change Research, Indian Institute of Tropical Meteorology, Pune, India

Received: 5 April 2015 – Accepted: 15 April 2015 – Published: 6 May 2015

Correspondence to: J. Sanjay (sanjay@tropmet.res.in)

Published by Copernicus Publications on behalf of the European Geosciences Union.

Abstract

Recent studies have drawn attention to a significant weakening trend of the South Asian monsoon circulation and an associated decrease in regional rainfall during the last few decades. While surface temperatures over the region have steadily risen during this period, most of the CMIP (Coupled Model Intercomparison Project) global climate models have difficulties in capturing the observed decrease of monsoon precipitation, thus limiting our understanding of the regional land surface response to monsoonal changes. This problem is investigated by performing two long-term simulation experiments, with and without anthropogenic forcing, using a variable resolution global climate model having high-resolution zooming over the South Asian region. The present results indicate that anthropogenic effects have considerably influenced the recent weakening of the monsoon circulation and decline of precipitation. It is seen that the simulated increase of surface temperature over the Indian region during the post-1950s is accompanied by a significant decrease of monsoon precipitation and soil moisture. Our analysis further reveals that the land surface response to decrease of soil moisture is associated with significant reduction in evapotranspiration over the Indian land region. A future projection, based on the representative concentration pathway 4.5 (RCP4.5) scenario of the Intergovernmental panel on Climate Change (IPCC), using the same high-resolution model indicates the possibility for detecting the summer-time soil drying signal over the Indian region during the 21st century, in response to climate change. While these monsoon hydrological changes have profound socioeconomic implications, the robustness of the high-resolution simulations provides deeper insights and enhances our understanding of the regional land surface response to the changing South Asian monsoon.

ESDD
6, 943–977, 2015

1 Introduction

The South Asian monsoon, also known as the Indian Summer Monsoon (ISM), brings approximately 70–80 % of the annual rainfall of the region during the season June–September (JJAS) and is the major source for water needs of the densely populated country. Any changes in the South Asian monsoon rainfall, which is a component of the larger-scale Asian monsoon system, due to climate change will have serious impacts on the socio-economic conditions of the country. Understanding the monsoon hydro-climatic response to climate change is also of great scientific interest. Several recent studies have reported significant negative trends in the observed seasonal monsoon precipitation on regional and sub-regional scales over South Asia since 1950s (e.g. Guhathakurta and Rajeevan, 2006; Chung and Ramanathan, 2006; Bollasina et al., 2011; Krishnan et al., 2013; Rajendran et al., 2012; Saha et al., 2014; Singh et al., 2014 and others). Various studies have also noted a weakening trend of the large-scale summer monsoon circulation during recent decades (e.g. Tanaka et al., 2004; Abish et al., 2013; Fan et al., 2010; Krishnan et al., 2013). Few modelling studies have attributed the climate forcing by aerosols as the major driver for the decreasing precipitation trend over the Indian region (see Chung and Ramanathan, 2006; Bollasina et al., 2011). There is also a view that rapid increase of moisture in a global warming environment can increase the atmospheric stability and weaken the tropical and monsoon circulations (e.g. Kitoh et al., 1997; Douville et al., 2000; Veechi et al., 2006; Ueda et al., 2006). High resolution model simulations reveal that a weakening of the south-westerly monsoon winds can in turn reduce orographic precipitation over the Western Ghat mountains (see Krishnan et al., 2013; Rajendran et al., 2012).

The land surface is an important component of the climate system that exchanges surface energy and hydrological fluxes with the atmosphere and influences the near surface climate. The role of evapotranspiration and soil moisture variations in influencing climate has been pointed out by several studies (Shukla and Mintz, 1982; Delworth and Manabe, 1988, 1989). Satellite derived soil moisture data from the Tropical Rainfall

ESDD
6, 943–977, 2015

Measuring Mission (TRMM) satellite during 1998–2008 indicates significant decreasing trends in soil moisture and evapotranspiration over many places globally and also over the Indian region (Jung et al., 2010). Using the terrestrial water storage observations from NASA Gravity Recovery and Climate Experiment satellites, Rodell et al. (2009) reported that the ground water in India is depleting at a faster rate than the rate of recovery. Kumar et al. (2013) noted an increasing trend in the intensity and percent area affected by moderate droughts during recent decades using a drought monitoring index viz., Standardized Precipitation Evapotranspiration Index (SPEI) which is based on climatic water balance.

Understanding the land surface and soil moisture response to anthropogenic forcing is important from scientific and societal perspectives, given their implications on climate, agriculture and other human activities (Seneviratne et al., 2006). One of the earliest investigations on the temporal and spatial variations of soil moisture response to global warming was conducted by Wetherald and Manabe (1999) using long-term integrations of a coupled atmosphere ocean global circulation model. Their results suggested that soil dryness due to global warming was prominently detectable over the mid-continental regions of middle and high latitudes by the end of first half of the 21st century. Over the Indian subcontinent, they noted an increase of soil moisture during the summer season due to increase of precipitation. However, these results were based on coarse resolution model simulations. Furthermore, models tend to exaggerate summer drying through overestimation of evaporation particularly in regions where soil moisture and energy are not limited (Seneviratne et al., 2002). Proper understanding of land-surface response over the Indian region to climate change is lacking due to poor simulation of monsoon precipitation in many coupled model intercomparison project (CMIP) models (Hasson et al., 2013). For example, Jourdain et al. (2013) reported a large spread in the simulated seasonal mean Indian summer monsoon rainfall as well as the seasonality of rainfall among the state-of-the-art CMIP5 coupled models used for the fifth Assessment Report of the Intergovernmental panel on Climate Change (IPCC). Also a majority of CMIP models do not adequately capture the his-

ESDD
6, 943–977, 2015

torical trend of decreasing precipitation over Indian monsoon region (e.g. Saha et al., 2014), with large uncertainties in future projections in the magnitude of monsoon precipitation over the region (Chaturvedi et al., 2012; Sharmila et al., 2015).

In this study, we have used a variable resolution global climate model from Laboratoire de Meterologie Dynamique (LMD), France with high-resolution (grid size < 35 km) telescopic zooming over South Asia and includes a state-of-the-art land-surface model, to better understand the regional land surface hydrological response to monsoonal changes. The model simulations also account for transient changes in land-use and land-cover, which are prescribed from standard datasets used in the CMIP5 experiments (see next section). Sabin et al. (2013) have assessed the South Asian monsoon simulations from the telescopically zoomed LMD model. They noted that the high-resolution LMD simulations provide important value additions in representing moist convective processes and organized convective activity over the monsoon region; and also realistically captured the regional details of precipitation characteristics and their links to monsoonal circulation. This paper is organised as follows. Section 2 provides a description of the model, design of experiments and observed data used for this work. Results from the historical simulations and comparison with observations are discussed in Sect. 3. The results of land hydrological response are presented in Sect. 4. The detectable future changes in land hydrology are described in Sect. 5 and the conclusions are summarized in Sect. 6.

2 Model, data and methods

2.1 Model and experiments

The climate model used in this study is the LMD global atmospheric general circulation model (AGCM) with enhanced resolution capability over a particular region of interest (see Hourdin et al., 2006; Sabin et al., 2013). The high resolution zoom used in this study is centred at 15° N, 80° E. The zoom domain (15° S–40° N, 30–120° E) covers

ESDD
6, 943–977, 2015

the entire South Asian monsoon region and the tropical Indian Ocean. The resolution is about 35 km in the zoom domain, and it becomes gradually coarser outside. Sabin et al. (2013) have evaluated different aspects of the South Asian monsoon simulation from this high-resolution model with telescopic zooming. The present version of LMDZ4 (Z stands for zoom; referred as LMDZ hereafter) GCM used in this study is based on a finite difference formulation of the primitive equations of meteorology, first described by Sadourny and Laval (1984). The dynamical equations are discretized on the sphere in a staggered and longitude–latitude Arakawa C-grid (Kasahara, 1977) with zooming capability. Discretization in the vertical is done by using a hybrid $\sigma - p$ coordinate system with 19 levels. The detailed description of the representation of physical processes in the version used here is given in Hourdin et al. (2006 and the references therein).

In this study, the LMDZ is coupled to a sophisticated land-surface model Organizing Carbon and Hydrology in Dynamic Ecosystems (ORCHIDEE; Krinner et al., 2005) for simulating land surface processes. The ORCHIDEE includes the full hydrological cycle and vegetation effects on energy, water and carbon fluxes. ORCHIDEE builds on the concept of plant functional types (PFT) to describe vegetation distributions. In ORCHIDEE, the land surface is represented as a heterogeneous mosaic of PFTs rather than discrete biomes, coexisting in a single grid. ORCHIDEE distinguishes 12 vegetation PFTs and one soil PFT. ORCHIDEE includes the surface parameterisation scheme, namely, Schématisation des Echanges Hydriques à L'Interface Biosphère– Atmosphère (SECHIBA; Ducoudré et al., 1993; de Rosnay and Polcher, 1998) to describe the exchange of energy and water between the atmosphere and the biosphere along with the soil water budget. In order to simulate the phenology and carbon dynamics of the terrestrial biosphere such as photosynthesis, carbon allocation, litter decomposition, soil carbon dynamics, respiration etc., ORCHIDEE uses a carbon module called STOMATE (Saclay Toulouse Orsay Model for the Analysis of Terrestrial Ecosystems). The vegetation distributions are prescribed according to the different model experiments, which will be discussed later.

ESDD
6, 943–977, 2015

The LMDZ AGCM with stretchable grids has been used for regional climate modeling studies over East Asian monsoon region (see Zhou and Li, 2002) and over the vicinity of Paris, France (Coindreau et al., 2007). Sabin et al. (2013) compared the South Asian monsoon simulation in the telescopically zoomed version against the no-zoom version of the model. They noted that the high-resolution zoomed simulation is more realistic as compared to the no-zoomed version in capturing the monsoon trough, various circulation features, the monsoon precipitation maximum along the narrow orography of the Western Ghat mountains, the north eastern mountain slopes and the northern Bay of Bengal.

We have conducted long-term simulation experiments using this configuration of the LMDZ GCM, with high-resolution (∼ 35 km) zooming over South Asia. These long-term simulation experiments follow CMIP5 (Taylor et al., 2012) framework, except with an AGCM. The first model simulation is the Historical run (HIST; 1886–2005), which uses both natural (e.g. Volcanoes, El Niño Southern Oscillation, ENSO) and anthropogenic (e.g. green house gases (GHG), aerosols evolution estimated from transport models, land use and land cover changes, etc.) forcing. The second experiment is Historical Natural run (NAT; 1886–2005), which uses only natural (e.g. Volcanoes, ENSO) forcing. Another simulation, which is intended to understand likely future changes (2006–2100), uses both natural and anthropogenic forcing based on IPCC approved medium stabilization scenario Representative Concentration Pathway 4.5 (RCP 4.5), in which the net radiative forcing at the end of 2100 is 4.5 $\mathrm{W\,m^{-2}}$.

The monthly bias adjusted SST and sea-ice from the corresponding CMIP5 coarser resolution Atmosphere Ocean coupled GCM run from Institut Pierre Simon Laplace (IPSL-CM5A-LR; referred as IPSL hereafter) are used as boundary forcing for LMDZ experiments. Bias adjustment refers to the removal of model errors in present day mean climate. First, we compute monthly SST anomalies for different IPSL model experiments relative to the monthly SST climatology derived from the historical simulation of IPSL for the period 1979–2005. These SST anomalies are then superposed on the observed climatological mean SST from the AMIP (Atmospheric Model Intercompar-

ESDD
6, 943–977, 2015

ison Project) dataset (http://www-pcmdi.llnl.gov/projects/amip/AMIP2EXPDSN/BCS/amip2bcs.php). The AMIP climatology is also computed for the same period 1979–2005. This approach retains the inter- and intra-annual variability and the climate change signal of the driving climate model. The same procedure is applied for specifying sea-ice boundary conditions.

The land use changes are prescribed using the historical crop and pasture datasets developed by Hurtt et al. (2011), which are also being used for the IPCC CMIP5 simulations. These datasets provide information on human activities (crop land and grazed pastureland) on a $0.5^{\circ} \times 0.5^{\circ}$ horizontal grid. The land-cover map used for both the historical and future period has been obtained starting from an observed present-day land-cover map (Loveland et al., 2000), which already includes both natural and anthropogenic vegetation types. These datasets are included in LMDZ following the methodology described by Dufresne et al. (2013).

2.2 Data

The model climate is compared with observational data to assess the model reliability. For this purpose we have used winds, precipitation and temperature data from observationally based and reanalysis estimates. The monthly circulation data at 850 and 200 hPa is obtained from a recent reanalysis produced by the European Centre for Medium-Range Weather Forecasts (ECMWF) called ERA-Interim (ERAI; Dee and Uppala, 2009; Dee et al., 2011) for the time period 1979–2005. Monthly Surface air temperature over land at the $0.5^{\circ} \times 0.5^{\circ}$ resolution from Climatic Research Unit (CRU TS3.1; Harris et al., 2014) for the period 1951–2005 is used. Precipitation observations over land from the Asian Precipitation – Highly-Resolved Observational Data Integration Towards Evaluation of Water Resources (APHRODITE) gridded ($0.5^{\circ} \times 0.5^{\circ}$) daily rainfall dataset (Yatagai et al., 2009) for the period 1951–2005 are used. In order to compare the model simulated precipitation over ocean regions, the observational based monthly precipitation data obtained from Climate Prediction Centre Merged Analysis of Precipitation (CMAP; Xie and Arkin, 1997) is also used. Monthly land surface hydro-

ESDD
6, 943–977, 2015

logical components from multiple off-line land model simulations of Global Land Data Assimilation System (GLDAS; Rodell et al., 2004) at 1° × 1° resolution are averaged to compute a multi-model mean and used to compare the model simulated land surface hydrological components by LMDZ as well as IPSL model from CMIP5 archive.

2.3 Methodology

The mean summer monsoon climate simulated by the LMDZ model is evaluated by comparing HIST simulation with different reanalysis and observational data sets for the parameters like circulation, 2 m temperature, precipitation and evapotranspiration. The added value of LMDZ high-resolution simulation is investigated by comparing with HIST simulation from the coarse-resolution IPSL coupled model. A 55 year period (1951–2005) of model simulations is chosen for the evaluation of mean climate of the models. It is to be noted that the time period considered for reanalyses data and CMAP precipitation (1979–2005) is different than that of model simulations (1951–2005). Pattern correlations are computed between different observational/reanalysed observational estimates and the model simulated fields to assess the model ability in capturing the large scale features of mean climate for different parameters. Observation grid is used as reference grid in the computation of pattern correlation, whereas in various figures we use the corresponding resolution for model and each data set. By comparing results from the two simulations HIST and NAT, the anthropogenic impact on mean summer monsoon hydrology is assessed. Linear trends are computed for the recent 55 year period of 1951–2005 for different variables like 2 m temperature, precipitation, soil moisture and evapotranspiration. Student *t* test is used to verify the significance of trends at 95 % level. The detectability of soil moisture changes in response to the anthropogenic forcing is assessed following Wetherald and Manabe (1999). The soil moisture changes are computed with respect to the long term mean (1886–2005) of NAT integration. The magnitudes of soil moisture changes are compared against the SD of the natural soil moisture variability in the NAT integration and the changes are considered to be detectable when they exceed the SD of the natural variability. The

ESDD
6, 943–977, 2015

same methodology is applied for other variables like 2 m air temperature and precipitation.

3 Model simulation of mean climate

3.1 Mean summer monsoon features

In this section, the simulations of the mean summer monsoon in the LMDZ model and the driving IPSL model are discussed and validated by comparison with reanalysis products and gridded observational estimates. Figure 1 shows the JJAS mean climatology of the lower (850 hPa) and upper (200 hPa) tropospheric wind circulation. The large-scale low level circulation features viz., the cross equatorial monsoon flow across the Indian Ocean, the Somali jet over the Arabian Sea and the monsoon trough over the Indian subcontinent can be noted in ERAI, the IPSL and LMDZ simulations (Fig. 1a–c). The wind climatology along the monsoon trough and head Bay of Bengal simulated by LMDZ is relatively closer to ERAI, as compared to the IPSL simulation. The pattern correlation between the simulated and observed low level wind climatology over the domain (20° S–35° N, 40–120° E) is 0.93 for LMDZ and 0.85 for the IPSL model. The major summer-time upper tropospheric wind circulation features such as the Tropical Easterly Jet over the Indian subcontinent, the Tibetan anticyclone and the subtropical westerly to the north of the subcontinent can be noted in ERAI and are captured in the IPSL and LMDZ simulations (Fig. 1d–f).

Figure 2 shows the spatial distributions of JJAS mean climatology of 2 m air temperature, precipitation and evapotranspiration (ET). The region of high temperatures with east–west orientation over northwest India and Pakistan (Fig. 2a) coincides with the monsoon trough and is better captured in the high-resolution LMDZ simulation (Fig. 2c) as compared to the IPSL coarse resolution model (Fig. 2b). The near surface air temperatures are underestimated both in LMDZ and IPSL simulations over central and peninsular India. The pattern correlations of the simulated and observed (CRU) mean surface air temperature over the land region (70–90° E, 10–28° N) are found to be 0.95 and 0.81 for the LMDZ and IPSL models respectively.

We also compared the simulated mean precipitation from the LMDZ and IPSL models with the CMAP and APHRODITE precipitation datasets over the Indian monsoon region. The CMAP is a merged precipitation gridded product obtained by combining satellite and rain gauge observations and is available both over land and oceanic regions on a 2.5° × 2.5° grid (Xie and Arkin, 1997). The APHRODITE is a high resolution 0.5° × 0.5° gridded rainfall dataset constructed from raingauge observations (Yatagai et al., 2012). The summer monsoon precipitation over central India and along the Indo Gangetic plains seen in the long term observed climatology from CMAP (Fig. 2d) are simulated relatively better in the LMDZ (Fig. 2f) model than the driving IPSL model (Fig. 2e), even though their magnitudes over these parts of India are lesser than the observed estimate. It is also found that the high resolution LMDZ model simulated rainfall maxima along the west coast, foot hills of Himalayas and northeast India are closer to high resolution rain gauge based observed climatology from APHRODITE (see Supplement Fig. S1). The pattern correlations of the simulated and observed (APHRODITE) mean precipitation over the Indian land region (70–90° E, 10–28° N) are found to be 0.47 and 0.20 for the LMDZ and IPSL models respectively.

The simulated evapotranspiration (ET), which is a major component of hydrological cycle, is compared with the GLDAS gridded dataset (Rodell et al., 2004). Observational uncertainties of surface hydrologic variables are large (Bindoff et al., 2013). The GLDAS dataset integrates observation based data to drive multiple off-line land surface models to generate flux parameters and land surface state (e.g. soil moisture, evapotranspiration, runoff, sensible heat flux, etc). Since the GLDAS off-line land surface models are driven by observations and bias-corrected reanalysis fields, the multi-model estimates from GLDAS serve as physically consistent reference datasets for model validation of land surface fluxes and state (Seneviratne et al., 2010). The JJAS mean evapotranspiration from GLDAS, the IPSL and LMDZ model simulations are shown in Fig. 2g–i. Note that the spatial distribution of the JJAS mean evapotranspiration from

ESDD
6, 943–977, 2015

GLDAS (Fig. 2g) has resemblance with the pattern of observed monsoon precipitation (Fig. 2d). The regions of high evapotranspiration over central, west coast of India and along foot hills of Himalayas are better simulated in the high resolution LMDZ as compared to the IPSL model (Fig. 2h–i). It is noted that the pattern correlations of ET between the simulated and GLDAS dataset over the Indian land region (70–90° E, 10–28° N) is 0.81for LMDZ and 0.58 for the coarse resolution IPSL model. The better ET distribution in the high resolution LMDZ simulation, as compared to the IPSL coarse resolution model, is consistent with simulated precipitation in the two models. Note that the orographic precipitation along the west coast of India and foot hills of Himalayas are better captured in LMDZ, whereas the IPSL model significantly underestimates rainfall over the Indian region resulting in low ET.

Here, we examine the annual water balance at surface in terms of precipitation, evapotranspiration and runoff from the LMDZ and IPSL simulations and validated with the GLDAS dataset (Fig. 3, Table 1). The pattern correlations of annual mean precipitation, evapotranspiration and runoff between the GLDAS dataset and the model simulations (LMDZ and IPSL) are shown in Table 1. It can be noted that the pattern correlation values for LMDZ are significantly higher than those of the IPSL model for all the three surface hydrological variables. Additionally, it is important to ensure model simulations properly capture surface water balances on regional scales. Hasson et al. (2013) noted that biases in simulating annual surface water balances on regional scale often introduce considerable uncertainty in assessment of surface hydrological response to climate change. Keeping this in view, we examined the difference of annual precipitation minus evapotranspiration ($P-\mathrm{ET}$) and the annual runoff averaged over the Indian land region (70.0–90.0° E; 10.0–28.0° N) from the GLDAS dataset and the two model simulations. The area-averaged values are shown in Table 2. It can be noticed that the annual ($P-\mathrm{ET}$) and runoff in GLDAS are in close balance (Table 2). A reasonably good balance between ($P-\mathrm{ET}$) and runoff can also be noted in the LMDZ simulation, whereas the annual runoff in the IPSL model far exceeds the ($P-\mathrm{ET}$). The fairly consistent balance between the annual ($P-\mathrm{ET}$) and runoff in the LMDZ model averaged

ESDD
6, 943–977, 2015

over the Indian region provides confidence in interpreting the land surface hydrological variations as compared to the IPSL coarse resolution model.

3.2 Simulation of climate trends over the monsoon region

A climate model's credibility is increased if the model is able to simulate past variations in climate, such as the trends over the twentieth century (Flato et al., 2013). The long-term drying trends (significant at > 95 % level) in the summer monsoon precipitation over parts of central India, along the Indo Gangetic plains and the narrow western ghat region during the past half century from APHRODITE (Fig. 4a) are captured with higher magnitudes in the HIST simulation of LMDZ (Fig. 4c) model. While the driving IPSL model (Fig. 4b), shows significant increasing trends in precipitation over most parts of India. The observed (CRU) significant warming trends over most parts of India (Fig. 5a) are captured by both simulations, with relatively larger magnitude in LMDZ (Fig. 5c) than IPSL (Fig. 5b) model. Further detailed analysis based on the LMDZ model experiment with only natural forcing (NAT) brings out the role of anthropogenic forcing on these drying and warming trends over India. The observed (APHRODITE) significant drying trends in summer monsoon precipitation over the Indian land region during 1951–2005 ($0.33\,\mathrm{mm\,d^{-1}(55\,yr)^{-1}}$) is only simulated by the HIST experiment of LMDZ model ($0.8\,\mathrm{mm\,d^{-1}(55\,yr)^{-1}}$) (Fig. S2b). The significant observed (CRU) seasonal warming trend for the same period ($0.5\,^{\circ}\mathrm{C}\,(55\,\mathrm{yr})^{-1}$) is also captured only by the HIST simulation of LMDZ model ($1.1\,^{\circ}\mathrm{C}\,(55\,\mathrm{yr})^{-1}$) (Fig. S2a). The surface air temperature and precipitation trends simulated in response to natural forcings only (NAT) are generally close to zero, and inconsistent with observed trends over Indian land region. These findings are further supported by the simulated weaker summer monsoon circulation and reduced precipitation over Indian subcontinent in the HIST experiment of LMDZ model compared to the NAT experiment (Fig. S3). The finding that the observed changes are consistent with the LMDZ simulation that include human influence (HIST), and are inconsistent with that do not (NAT) would be sufficient for attribution studies as they typically assume that models simulate the large-scale spatial and temporal

ESDD
6, 943–977, 2015

patterns of the response to external forcing correctly, but do not assume that models simulate the magnitude of the response correctly (Bindoff et al., 2013). Hence this high-resolution HIST simulation of LMDZ model will be an important value addition for understanding the regional land surface hydrological responses due to anthropogenic forced changes in summer monsoon over the Indian subcontinent.

4 Response of land surface hydrology to the changing monsoon

We further assess the long-term changes in the surface hydrologic variables such as soil moisture (SM) and ET in the HIST simulation of LMDZ. In association with the reduction of summer monsoon precipitation, the HIST simulation of LMDZ model also indicate significant soil moisture (SM) drying trends over most parts of India (Fig. 6a). This accounts to about 14 mm $(55\,\mathrm{yr})^{-1}$ reduction in soil moisture (5 %) when area averaged over the Indian land region. The comparison of the seasonal trends at each grid point over the Indian land region indicates a dominant control of precipitation on SM (Fig. S4). The SM is a source of water for the atmosphere through processes leading to ET from land, which include mainly plant transpiration and bare soil evaporation. The HIST simulation of LMDZ model show significant decrease of summer season mean ET over most parts of the Indian land region (Fig. 6b). The Indian land region area averaged reduction in ET accounts for about 0.23 $\mathrm{mm\,d^{-1}}(55\,\mathrm{yr})^{-1}$ (9.5 %). The simulated regions of ET reduction mostly coincide with that of drier soil moisture.

The global hydrological cycle is generally expected to intensify in a warming world, leading to increase in ET (Huntington, 2006). On the other hand, station observations of pan evaporation over India indicate a significant decreasing trend in recent decades (Padmakumari et al., 2013). Long-term trends in ET are basically driven by limiting factors such as soil moisture or radiation both on regional (Teuling et al., 2009) and global (Jung et al., 2010) scales. A comparison of the simulated seasonal ET trends at each grid point over Indian land region with the corresponding SM trends shows significant correlation between ET reduction and SM drying (Fig. 7a). This relationship is also noticed under conditions of increasing and decreasing surface incident solar radiation trends (Fig. 7b and c), implying that SM drying plays a dominant role in ET reduction over the Indian monsoon region, with minor contributions from changes in solar radiation reaching at surface. In fact, it can be noticed from Fig. 7b that decrease of ET is mostly accompanied by decrease of SM over a majority of grid-points over the Indian region, whereas increases in ET and global radiation are seen over fewer grid-points. The above analysis suggests that the SM drying trends, caused by local precipitation variations, largely drive ET reduction over the region.

5 Future changes in surface hydrology

The spatial distributions of the projected future trends in temperature, precipitation, soil moisture and evapotranspiration for the period 2006–2095 under RCP 4.5 scenario are shown in Fig. 8. The significant increase of temperature over the entire Indian land region is consistent with the increasing radiative effects of the rising CO_2 concentration in the future (Fig. 8a). The magnitude of this warming is larger (1.5–2 °C) at northern regions including Indo Gangetic planes and smaller along the western regions and the southern most parts of India. The projected future trends in precipitation show regions of significant increase over western and south eastern parts and decrease over Central India (Fig. 8b). Note that the spatial pattern of trends in SM mostly follows the pattern of precipitation trends and is dominated by drying of SM (Fig. 8c). It is also interesting to note that the spatial pattern of projected trends in ET resembles the pattern of trends in SM (Fig. 8d).

The detectability of soil moisture changes to anthropogenic forcing is computed following the approach of Wetherald and Manabe (1999). The magnitudes of soil moisture changes with respect to the long term mean (1886–2005) of NAT integration are compared against the SD of the natural soil moisture variability in the NAT integration. The changes are considered to be detectable when they exceed the SD of the natural variability. For this analysis, we sequentially arrange variables for the HIST time

ESDD
6, 943–977, 2015

period (1886–2005) and RCP4.5 scenario (2006–2095) as a continuous time-series, which will be henceforth referred to as ALL. Figure 9a shows the smoothed time-series of 20 year running-mean values of summer-monsoon soil moisture anomalies during 1886–2095 based on the high-resolution (LMDZ) and coarse-resolution (IPSL) simulations over the Central Indian region (74.5–86.5° E; 16.5–26.5° N; see box in Fig. 8a). The SD of soil moisture in Fig. 9a is calculated from the corresponding natural (NAT) integrations. The appearance of a detectable change of soil moisture (exceeding one SD of NAT) can be noted in the LMDZ simulation as early as 2010 and continues till the end of the 21st century. On the other hand, the SM variations in the IPSL simulation show decadal-scale variations with slight decrease during latter part of the 21st century. Here, it is important to note that the surface warming trend during (1886–2005) is clearly borne out in both the IPSL and LMDZ models (Fig. 9b), with the magnitude of warming trend being more pronounced in the LMDZ simulation (0.21 $\mathrm{K\,decade^{-1}}$) as compared to the IPSL model (0.15 $\mathrm{K\,decade^{-1}}$). The appearance of a detectable change of soil moisture lags behind that of surface air temperature by several decades. This is due to the relatively smaller signal-to-noise ratio for soil moisture variability as compared to that of the surface air temperature (see Delworth and Manabe, 1989). Furthermore, the smaller signal-to-noise ratio of soil moisture over the Indian region indicates relatively large natural interannual variability of summer monsoon precipitation (Fig. 9c). The IPSL model projection shows enhancement of monsoon precipitation and increase of soil moisture by the end of the 21st century (Fig. 9a and c). The decrease in monsoon precipitation over central India in the high-resolution LMDZ simulation is noticeable by early 21st century. It is also interesting to see that the high resolution simulation indicates decrease of soil moisture from middle to the end of 21st century over central India, despite a gradual revival of the projected monsoon precipitation by the mid 21st century. From the above discussion, it is seen that the high-resolution LMDZ simulations provide important value additions in terms of regional land surface response to changes in the South Asian monsoon.

ESDD
6, 943–977, 2015

6 Conclusions

We have used a state-of-the-art global climate model (LMDZ), with high-resolution telescopic zooming over South Asia, to investigate the regional land-surface response to changing climate and declining summer monsoon rains observed during the last few decades. This high-resolution climate model captures well the distribution of the mean monsoon rainfall and circulation features (Sabin et al., 2013). It is also noted that the high-resolution LMDZ model, which is coupled to a sophisticated land-surface parameterization scheme, displays a consistent surface water balance over the South Asian region – which is essential for making reliable assessments of the regional hydrological response to monsoonal changes. In the present work, we have performed two long-term simulation experiments, with and without anthropogenic forcing, for the historical period 1886–2005; and one future projection following the RCP4.5 scenario.

The results from our study suggest that the declining trend of monsoon precipitation over South Asia and weakening of large-scale summer monsoon circulation during the post-1950s are largely attributable to anthropogenic forcing. It is found that the model simulated response to anthropogenic forcing shows an increase of surface temperature over the India region at a rate of 1.1 °C $(55\,\text{yr})^{-1}$, a decline of summer monsoon precipitation at a rate of 0.8 $\text{mm}\,\text{d}^{-1}(55\,\text{yr})^{-1}$ and a corresponding reduction of soil moisture at a rate of 14 $\text{mm}\,(55\,\text{yr})^{-1}$. The simulated decrease of mean monsoon precipitation over the Indian region during the post-1950s is accompanied by a weakening of large-scale monsoon circulation and is consistent with observations. The results of a future climate projection using medium scenario (RCP 4.5) shows likely continuation of the drying trend in monsoon rainfall and noticeable decrease of soil moisture till the end of the 21st century. The present high-resolution simulations are scientifically interesting, particularly given that the CMIP5 models driven with same scenario generally show a slight increase in mean precipitation over the Indian region, associated with large uncertainties (Chaturvedi et al., 2012).

ESDD
6, 943–977, 2015

The declining monsoonal rains and the associated hydro-climatic changes can have profound implications for crop production and socio-economic activities in the region. Our findings from the high-resolution LMDZ simulations suggest that persistent decrease of monsoon rainfall and soil moisture over the Indian region has significant impact on the regional land surface hydrology. The simulations show that a decrease of soil moisture over the Indian land region by 5 % during 1951–2005 is accompanied by a decrease of ET by 9.5 %. It is noticed that the ET reduction and SM drying, over the Indian land points, are significantly correlated even under conditions of increasing surface incident short wave radiation trends, implying that SM drying plays a dominant role in ET reduction in the region. While this study is based on a single realization, the realism of the high resolution simulation enhances our confidence in interpreting the land-surface hydrological response to climate change and declining monsoons. We realize that a suite of ensemble simulations will be required for quantifying uncertainties in the land surface hydrological response to monsoonal changes. This is a topic of future research and beyond the scope of the present study.

The Supplement related to this article is available online at doi:10.5194/esdd-6-943-2015-supplement.

Acknowledgements. Authors thank Director IITM for extending all support for this research work. IITM is supported by Ministry of Earth Sciences, Government of India, New Delhi. The figures are prepared using GrADS. M. V. S. Ramarao is financially supported by the Indian Institute for Human Settlements (IIHS) through the Adaptation at Scale in Semi-Arid Regions (ASSAR) consortia of the Collaborative Adaptation Research initiative in Africa and Asia (CARIAA). We acknowledge the World Climate Research Programme's Working Group on Coupled Modeling, which is responsible for CMIP, and we thank the IPSL climate modeling group for producing and making available their model output.

References

Abish, B., Joseph, P. V., and Johannessen, O. M.: Weakening trend of the tropical easterly jet stream of the boreal summer monsoon season 1950–2009, J. Climate, 26, 9408–9414, doi:10.1175/JCLI-D-13-00440.1, 2013.

Bindoff, N. L., Stott, P., AchutaRao, K., Allen, M., Gillett, N., Gutzler, D., Hansingo, K., Hegerl, G., Hu, Y., Jain, S., Mokhov, I., Overland, J., Perlwitz, J., Sebbari, R., and Zhang, X.: Detection and Attribution of Climate Change: from Global to Regional, in: Climate Change 2013: The Physical Science Basis, Contribution of Working Group I to the Fifth Assessment Report of the Intergovernmental Panel on Climate Change, edited by: Stocker, T. F., Qin, D., Plattner, G.-K., Tignor, M., Allen, S. K., Boschung, J., Nauels, A., Xia, Y., Bex, V., and Midgley, P. M., Cambridge University Press, Cambridge, UK and New York, NY, USA, 867–952, 2013.

Bollasina, M. A., Ming, Y., and Ramaswamy, V.: Anthropogenic aerosols and the weakening of the South Asian Summer Monsoon, Science, 334, 502–505, doi:10.1126/science.1204994, 2011.

Chaturvedi, R. K., Joshi, J., Jayaraman, M., Bala, G., and Ravindranath, N. H.: Multi-model climate change projections for India under representative concentration pathways, Current Sci., 103, 791–802, 2012.

Chung, C. E. and Ramanathan, V.: Weakening of north Indian SST gradients and the monsoon rainfall in India and the Sahel, J. Climate, 19, 2036–2045, doi:10.1175/JCLI3820.1, 2006.

Coindreau, O., Hourdin, F., Haeffelin, M., Mathieu, A., and Rio, C.: Assessment of physical parameterizations using a global climate model with stretchable grid and nudging, Mon. Weather Rev., 135, 1474–1489, doi:10.1175/MWR3338.1, 2007.

Dee, D. P. and Uppala, S.: Variational bias correction of satellite radiance data in the ERA-Interim reanalysis, Q. J. Roy. Meteorol. Soc., 135, 1830–1841, doi:10.1002/qj.493, 2009.

Dee, D. P., Uppala, S. M., Simmons, A. J., Berrisford, P., Poli, P., Kobayashi, S., Andrae, U., Balmaseda, M. A., Balsamo, G., Bauer, P., Bechtold, P., Beljaars, A. C. M., van de Berg, L., Bidlot, J., Bormann, N., Delsol, C., Dragani, R., Fuentes, M., Geer, A. J., Haimberger, L., Healy, S. B., Hersbach, H., Hólm, E. V., Isaksen, L., Kållberg, P., Köhler, M., Matricardi, M., McNally, A. P., Monge-Sanz, B. M., Morcrette, J.-J., Park, B.-K., Peubey, C., de Rosnay, P., Tavolato, C., Thépaut, J.-N. and Vitart, F.: The ERA-Interim reanalysis: configuration and performance of the data assimilation system, Q. J. Roy. Meteorol. Soc., 137, 553–597, doi:10.1002/qj.828, 2011.

Delworth, T. L. and Manabe, S.: The influence of potential evaporation on the variabilities of simulated soil wetness and climate, J. Climate, 1, 523–547, 1988.
Delworth, T. L. and Manabe, S.: The Influence of soil wetness on near-surface atmospheric variability, J. Climate, 2, 1447–1462, 1989.
de Rosnay, P. and Polcher, J.: Modelling root water uptake in a complex land surface scheme coupled to a GCM, Hydrol. Earth Syst. Sci., 2, 239–255, doi:10.5194/hess-2-239-1998, 1998.
Ducoudré, N. I., Laval, K., and Perrier, A.: SECHIBA, a new set of parameterizations of the hydrologic exchanges at the land–atmosphere interface within the LMD Atmospheric General Circulation Model, J. Climate, 6, 248–273, doi:10.1175/1520-0442(1993)006<0248:SANSOP>2.0.CO;2, 1993.
Dufresne, J.-L., Foujols, M.-A., Denvil, S., Caubel, A., Marti, O., Aumont, O., Balkanski, Y., Bekki, S., Bellenger, H., Benshila, R., Bony, S., Bopp, L., Braconnot, P., Brockmann, P., Cadule, P., Cheruy, F., Codron, F., Cozic, A., Cugnet, D., de Noblet, N., Duvel, J.-P., Ethé, C., Fairhead, L., Fichefet, T., Flavoni, S., Friedlingstein, P., Grandpeix, J.-Y., Guez, L., Guilyardi, E., Hauglustaine, D., Hourdin, F., Idelkadi, A., Ghattas, J., Joussaume, S., Kageyama, M., Krinner, G., Labetoulle, S., Lahellec, A., Lefebvre, M.-P., Lefevre, F., Levy, C., Li, Z. X., Lloyd, J., Lott, F., Madec, G., Mancip, M., Marchand, M., Masson, S., Meurdesoif, Y., Mignot, J., Musat, I., Parouty, S., Polcher, J., Rio, C., Schulz, M., Swingedouw, D., Szopa, S., Talandier, C., Terray, P., Viovy, N., and Vuichard, N.: Climate change projections using the IPSL-CM5 Earth System Model: from CMIP3 to CMIP5, Clim. Dynam., 40, 2123–2165, doi:10.1007/s00382-012-1636-1, 2013.
Douville, H., Royer, J.-F., Polcher, J., Cox, P., Gedney, N., Stephenson, D. B., and Valdes, P. J.: Impact of doubling CO_2 on the Asian summer monsoon: robust vs. model-dependent responses, J. Meteorol. Soc. Jpn., 78, 421–439, 2000.
Fan, F., Mann, M. E., Lee, S., and Evans, J. L.: Observed and modeled changes in the South Asian summer monsoon over the historical period, J. Climate, 23, 5193–5205, doi:10.1175/2010JCLI3374.1, 2010.
Flato, G., Marotzke, J., Abiodun, B., Braconnot, P., Chou, S. C., Collins, W., Cox, P., Driouech, F., Emori, S., Eyring, V., Forest, C., Gleckler, P., Guilyardi, E., Jakob, C., Kattsov, V., Reason, C., and Rummukainen, M.: Evaluation of Climate Models, in: Climate Change 2013: The Physical Science Basis, Contribution of Working Group I to the Fifth Assessment Report of the Intergovernmental Panel on Climate Change, edited by: Stocker, T. F., Qin, D.,

ESDD
6, 943–977, 2015

Understanding land surface response to changing South Asian monsoon in a warming climate

M. V. S. Ramarao et al.

Plattner, G.-K., Tignor, M., Allen, S. K., Boschung, J., Nauels, A., Xia, Y., Bex, V., and Midgley, P. M., Cambridge University Press, Cambridge, UK and New York, NY, USA, 741–866, doi:10.1017/CBO9781107415324.020, 2013.

Guhathakurta, P. and Rajeevan, M.: Trends in the rainfall pattern over India, National climate Centre (NCC) Research Report No. 2, India. Met. Department., Pune, 1–23, 2006.

Harris, I., Jones. P. D., Osborn, T. J., and Lister, D. H.: Updated high-resolution grids of monthly climatic observations – the CRU TS3.10 Dataset, Int. J. Climatol., 34, 623–642, doi:10.1002/joc.3711, 2014.

Hasson, S., Lucarini, V., and Pascale, S.: Hydrological cycle over South and Southeast Asian river basins as simulated by PCMDI/CMIP3 experiments, Earth Syst. Dynam., 4, 199–217, doi:10.5194/esd-4-199-2013, 2013.

Hourdin, F., Musat, I., Bony, S., Braconnot, P., Codron, F., Dufresne, J. L., Fairhead, L., Filiberti, M. A., Friedlingstein, P., Grandpeix, J. Y., Krinner, G., LeVan, P., Li, Z. X., and Lott, F.: The LMDZ4 general circulation model: climate performance and sensitivity to parametrized physics with emphasis on tropical convection, Clim. Dynam., 27, 787–813, doi:10.1007/s00382-006-0158-0, 2006.

Huntington, T. G.: Evidence for intensification of the global water cycle: review and synthesis, J. Hydrol., 319, 83–95, 2006.

Hurtt, G., Chini, L., Frolking, S., Betts, R., Feddema, J., Fischer, G., Fisk, J., Hibbard, K., Houghton, R., Janetos, A., Jones, C., Kindermann, G., Kinoshita, T., Klein Goldewijk, K., Riahi, K., Shevliakova, E., Smith, S., Stehfest, E., Thomson, A., Thornton, P., van Vuuren, D., and Wang, Y.: Harmonization of land-use scenarios for the period 1500–2100: 600 years of global gridded annual land-use transitions, wood harvest, and resulting secondary lands, Climatic Change, 109, 117–161, doi:10.1007/s10584-011-0153-2, 2011.

Jourdain, N. C., Gupta, A. Sen, Taschetto, A. S., Ummenhofer, C. C., Moise, A. F., and Ashok, K.: The Indo-Australian monsoon and its relationship to ENSO and IOD in reanalysis data and the CMIP3/CMIP5 simulations, Clim. Dynam., 41, 3073–3102, doi:10.1007/s00382-013-1676-1, 2013.

Jung, M., Reichstein, M., Ciais, P., Seneviratne, S. I., Sheffield, J., Goulden, M. L., Bonan, G., Cescatti, A., Chen, J., de Jeu, R., Dolman, A. J., Eugster, W., Gerten, D., Gianelle, D., Gobron, N., Heinke, J., Kimball, J., Law, B. E., Montagnani, L., Mu, Q., Mueller, B., Oleson, K., Papale, D., Richardson, A. D., Roupsard, O., Running, S., Tomelleri, E., Viovy, N., Weber, U., Williams, C., Wood, E., Zaehle, S., and Zhang, K.: Recent decline in the

ESDD

6, 943–977, 2015

global land evapotranspiration trend due to limited moisture supply, Nature, 467, 951–954, doi:10.1038/nature09396, 2010.

Kasahara, A.: Computational aspects of numerical models for weather prediction and climate simulation, in: Methods in Computational Physics, Vol. 17, edited by: Chang, J., Academic, Amsterdam, 1–66, 1977.

Kitoh, A., Yukimoto, S., Noda, A., and Motoi, T.: Simulated changes in the Asian summer monsoon at times of increased atmospheric CO_2, J. Meteorol. Soc. Jpn., 75, 1019–1031, 1997.

Krinner, G., Viovy, N., de Noblet-Ducoudré, N., Ogée, J., Polcher, J., Friedlingstein, P., Ciais, P., Sitch, S., and Prentice, C.: A dynamic global vegetation model for studies of the coupled atmosphere–biosphere system, Global Biogeochem. Cy., 19, GB1015, doi:10.1029/2003GB002199, 2005.

Krishnan, R., Sabin, T. P., Ayantika, D. C., Kitoh, A., Sugi, M., Murakami, H., Turner, A. G., Slingo, J. M., and Rajendran, K.: Will the South Asian monsoon overturning circulation stabilize any further?, Clim. Dynam., 40, 187–211, doi:10.1007/s00382-012-1317-0, 2013.

Kumar, K. N., Rajeevan, M., Pai, D. S., Srivastava, A. K., and Preethi, B.: On the observed variability of monsoon droughts over India, Weather Clim. Extrem., 1, 42–50, doi:10.1016/j.wace.2013.07.006, 2013.

Loveland, T. R., Reed, B. C., Brown, J. F., Ohlen, D. O., Zhu, Z., Yang, L., and Merchant, J. W.: Development of a global land cover characteristics database and IGBP DISCover from 1 km AVHRR data, Int. J. Remote. Sens., 21, 1303–1330, doi:10.1080/014311600210191, 2000.

Padmakumari, B., Jaswal, A. K., and Goswami, B. N.: Decrease in evaporation over the Indian monsoon region: implication on regional hydrological cycle, Climatic Change, 121, 787–799, doi:10.1007/s10584-013-0957-3, 2013.

Rajendran, K., Kitoh, A., Srinivasan, J., Mizuta, R., and Krishnan, R.: Monsoon circulation interaction with Western Ghats orography under changing climate projection by a 20 km mesh AGCM, Theor. Appl. Climatol., 110, 555–571, doi:10.1007/s00704-012-0690-2, 2012.

Rodell, M., Houser, P. R., Jambor, U., Gottschalck, J., Mitchell, K., Meng, C.-J., Arsenault, K., Cosgrove, B., Radakovich, J., Bosilovich, M., Entin, J. K., Walker, J. P., Lohmann, D. and Toll, D.: The Global Land Data Assimilation System, B. Am. Meteorol. Soc., 85, 381–394, 2004.

Rodell, M., Velicogna, I., and Famiglietti, J. S.: Satellite-based estimates of groundwater depletion in India, Nature, 460, 999–1002, doi:10.1038/nature08238, 2009.

ESDD

6, 943–977, 2015

Understanding land surface response to changing South Asian monsoon in a warming climate

M. V. S. Ramarao et al.

Sabin, T. P., Krishnan, R., Ghattas, J., Denvil, S., Dufresne, J. L., Hourdin, F., and Pascal, T.: High resolution simulation of the South Asian monsoon using a variable resolution global climate model, Clim. Dynam., 41, 173–194, doi:10.1007/s00382-012-1658-8, 2013.

Sadourny, R. and Laval, K.: January and July performance of the LMD general circulation model, in: New Perspectives in Climate Modeling, edited by: Berger, A. and Nicolis, C., Elsevier, Amsterdam, 173–197, 1984.

Saha, A., Ghosh, S., Sahana, A. S., and Rao, E. P.: Failure of CMIP5 climate models in simulating post-1950 decreasing trend of Indian monsoon, Geophys. Res. Lett., 41, 7323–7330, doi:10.1002/2014GL061573, 2014.

Seneviratne, S. I., Pal, J. S., Eltahir, E. A. B., and Schär, C.: Summer dryness in a warmer climate: a process study with a regional climate model, Clim. Dynam., 20, 69–85, doi:10.1007/s00382-002-0258-4, 2002.

Seneviratne, S. I., Lüthi, D., Litschi, M., and Schär, C.: Land–atmosphere coupling and climate change in Europe, Nature, 443, 205–209, doi:10.1038/nature05095, 2006.

Seneviratne, S. I., Corti, T., Davin, E. L., Hirschi, M., Jaeger, E. B., Lehner, I., Orlowsky, B., and Teuling, A. J.: Investigating soil moisture-climate interactions in a changing climate: a review, Earth-Sci. Rev., 99, 125–161, doi:10.1016/j.earscirev.2010.02.004, 2010.

Sharmila, S., Joseph, S., Sahai, A. K., Abhilash, S., and Chattopadhyay, R.: Future projection of Indian summer monsoon variability under climate change scenario: an assessment from CMIP5 climate models, Global Planet. Change, 124, 62–78, doi:10.1016/j.gloplacha.2014.11.004, 2015.

Shukla, J. and Mintz, Y.: The influence of land-surface evapotranspiration on the Earth's climate, Science, 214, 1498–1501, 1982.

Singh, D., Tsiang, M., Rajaratnam, B., and Diffenbaugh, N. S.: Observed changes in extreme wet and dry spells during the South Asian summer monsoon season, Nat. Clim. Change, 4, 1–6, doi:10.1038/nclimate2208, 2014.

Tanaka, H. L., Ishizaki, N., and Kitoh, A.: Trend and interannual variability of Walker, monsoon and Hadley circulations defined by velocity potential in the upper troposphere, Tellus A, 56, 250–269, 2004.

Taylor, K. E., Stouffer, R. J., and Meehl, G. A.: An overview of CMIP5 and the experiment design, B. Am. Meteorol. Soc., 93, 485–498, doi:10.1175/BAMS-D-11-00094.1, 2012.

Teuling, A. J., Hirschi, M., Ohmura, A., Wild, M., Reichstein, M., Ciais, P., Buchmann, N., Ammann, C., Montagnani, L., Richardson, A. D., Wohlfahrt, G., and Seneviratne, S. I.: A

ESDD
6, 943–977, 2015

Understanding land surface response to changing South Asian monsoon in a warming climate

M. V. S. Ramarao et al.

regional perspective on trends in continental evaporation, Geophys. Res. Lett., 36, 1–5, doi:10.1029/2008GL036584, 2009.

Ueda, H., Iwai, A., Kuwako, K., and Hori, M. E.: Impact of anthropogenic forcing on the Asian summer monsoon as simulated by eight GCMs, Geophys. Res. Lett., 33, L06703, doi:10.1029/2005GL025336, 2006.

Veechi, G. A., Soden, B. J., Wittenberg, A. T., Held, I. M., Leetma, A., and Harrison, M. J.: Weakening of tropical Pacific atmospheric circulation due to anthropogenic forcing, Nature, 441, 73–76, 2006.

Wetherald, R. T. and Manabe, S.: Detectability of summer dryness caused by greenhouse warming, Climatic Change, 43, 495–511, 1999.

Xie, P. and Arkin, P. A.: Global precipitation: a 17 year monthly analysis based on gauge observations, satellite estimates, and numerical model outputs, B. Am. Meteorol. Soc., 78, 2539–2558, 1997.

Yatagai, A., Kamiguchi, K., Arakawa, O., Hamada, A., Yasutomi, N., and Kitoh, A.: APHRODITE: constructing a long-term daily gridded precipitation dataset for Asia based on a dense network of rain gauges, B. Am. Meteorol. Soc., 93, 1401–1415, doi:10.1175/BAMS-D-11-00122.1, 2012.

Zhou, T. and Li, Z.: Simulation of the East Asian summer monsoon using a variable resolution atmospheric GCM, Clim. Dynam., 19, 167–180, 2002.

ESDD

6, 943–977, 2015

Understanding land surface response to changing South Asian monsoon in a warming climate

M. V. S. Ramarao et al.

Table 1. Pattern correlations for annual mean climatology of precipitation (P), evapotranspiration (ET) and runoff (R) from IPSL and LMDZ with GLDAS.

	IPSL	LMDZ
P	0.4	0.56
ET	0.74	0.84
R	0.2	0.34

ESDD
6, 943–977, 2015

Table 2. Long term annual means in mm d^{-1} for precipitation (P), Evapotranspiration (ET), runoff (R) and P – ET from GLDAS, IPSL and LMDZ models during 1979–2005 averaged over the domain 70–90° E; 10–28° N. The water balance is highlighted.

	GLDAS	IPSL	LMDZ
P	2.63	1.81	2.97
ET	1.99	2.25	1.92
R	**0.65**	**0.28**	**1.06**
P – ET	**0.64**	**–0.44**	**1.05**

ESDD
6, 943–977, 2015

ESDD
6, 943–977, 2015

Understanding land surface response to changing South Asian monsoon in a warming climate

M. V. S. Ramarao et al.

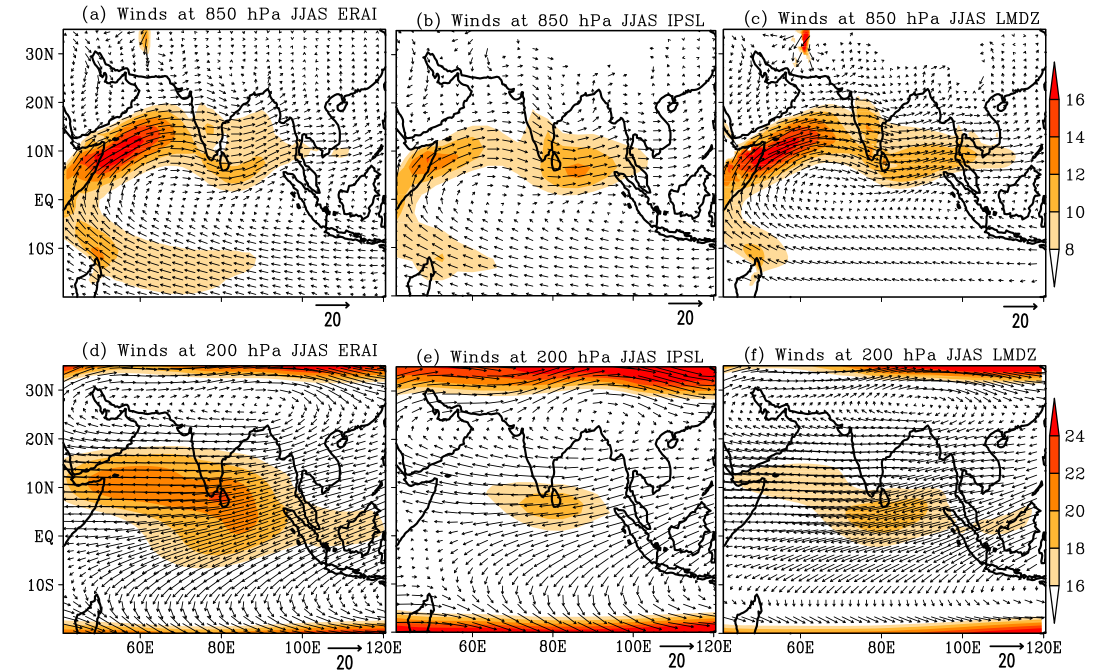

Figure 1. Spatial maps for JJAS mean wind fields ($m\,s^{-1}$) at (top panels) 850 hPa and (bottom panels) 200 hPa for **(a, d)** ERAI, **(b, e)** IPSL and **(c, f)** LMDZ simulations. Shading denotes wind magnitude.

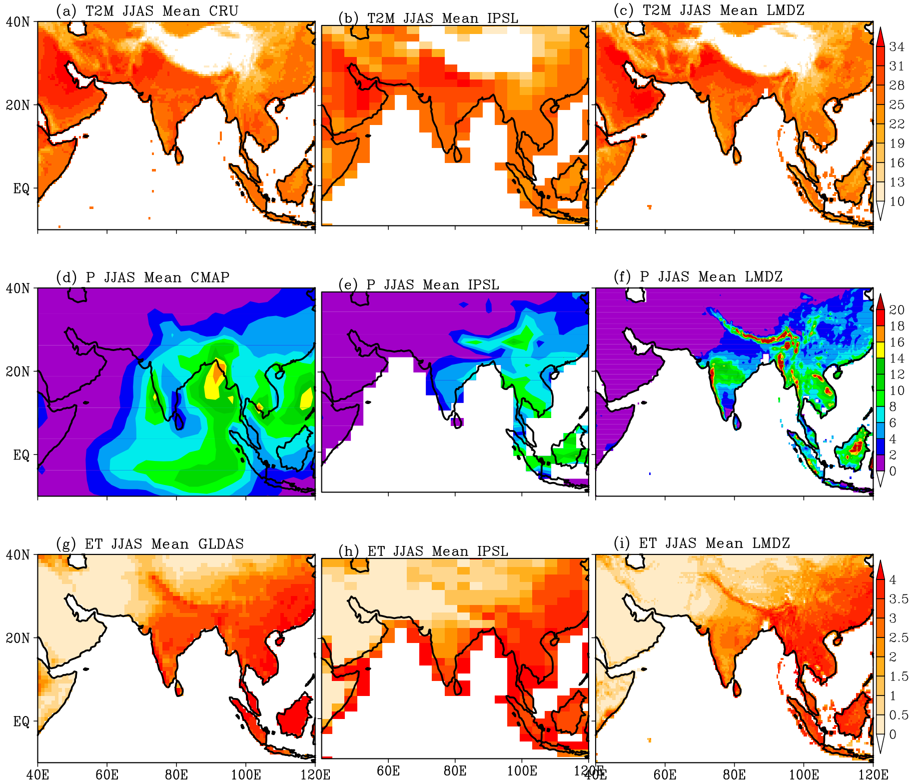

Figure 2. Spatial distributions of JJAS mean (top panels) 2 m air temperature (T2M; °C), (middle panels) precipitation (P; mm d^{-1}) and (bottom panels) evapotranspiration (ET; mm d^{-1}) from **(a, d ,g)** observations/multi model data, from HIST simulations of **(b, e, h)** IPSL and **(c, f, i)** LMDZ models.

ESDD
6, 943–977, 2015

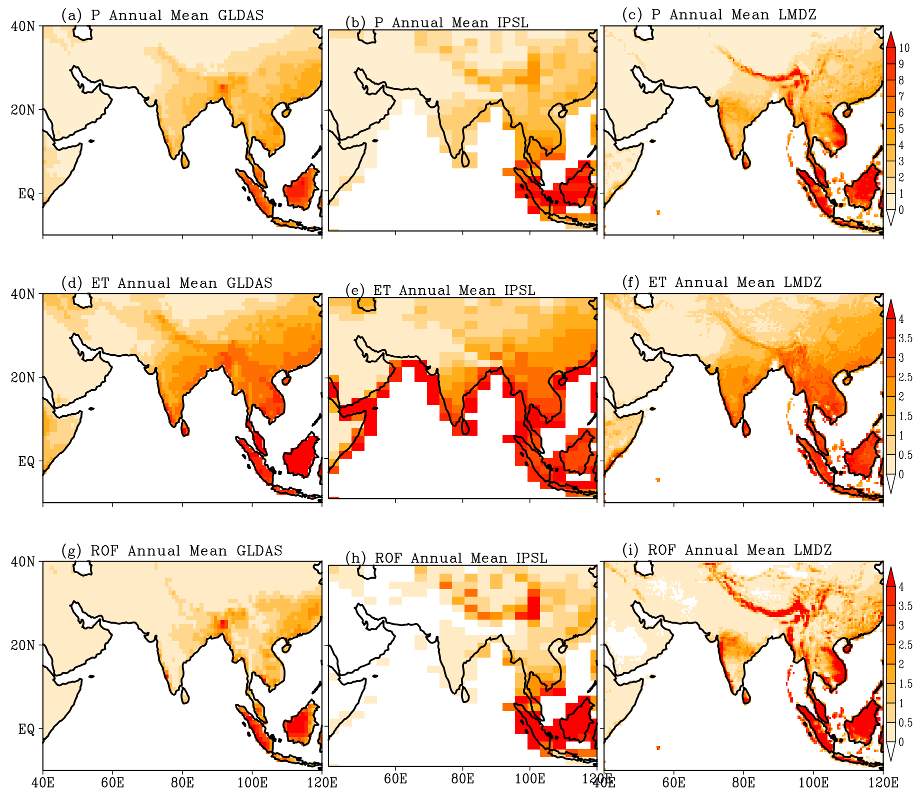

Figure 3. Spatial maps for annual mean (top panels) precipitation, (middle panels) evapotranspiration and (bottom panels) runoff from **(a, d, g)** GLDAS, **(b, e, h)** IPSL and **(c, f, i)** LMDZ simulations during 1979–2005. Units are mm d^{-1}.

ESDD
6, 943–977, 2015

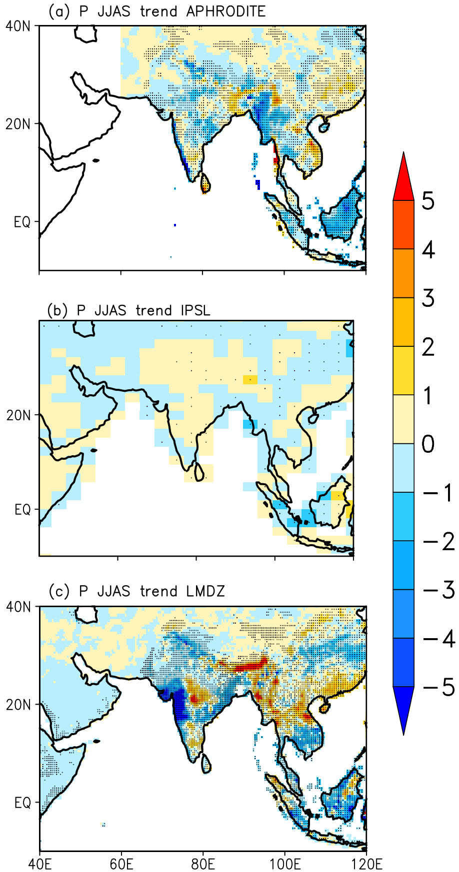

Figure 4. Spatial maps of linear trends in JJAS rainfall based on **(a)** APHRODITE, **(b)** IPSL and **(c)** LMDZ HIST simulation. Units are $\mathrm{mm\,d^{-1}}$ change over the period 1951–2005. Trend values exceeding the 95 % level of statistical significance based on Students t test are stippled.

ESDD
6, 943–977, 2015

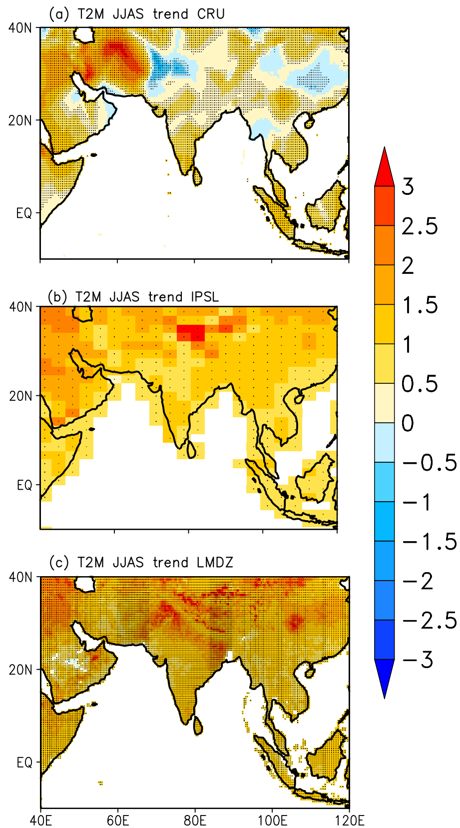

Figure 5. Spatial maps of linear trends in 2 m air temperature for JJAS season based on **(a)** CRU, **(b)** IPSL and **(c)** LMDZ HIST simulation. Units are °C change over the period 1951–2005. Trend values exceeding the 95 % level of statistical significance based on Students *t* test are stippled.

ESDD
6, 943–977, 2015

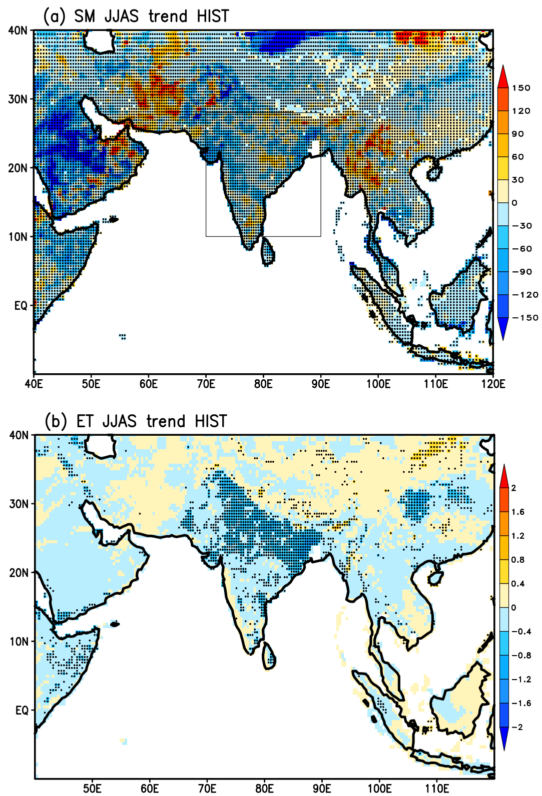

Figure 6. Spatial distribution of linear trends in JJAS mean **(a)** total soil moisture (SM) and evapotranspiration (ET) from HIST simulation of LMDZ. Units are mm and mm d^{-1} change over the period 1951–2005 for SM and ET respectively. Trend values exceeding the 95 % level of statistical significance based on Students t test are stippled.

ESDD
6, 943–977, 2015

Understanding land surface response to changing South Asian monsoon in a warming climate

M. V. S. Ramarao et al.

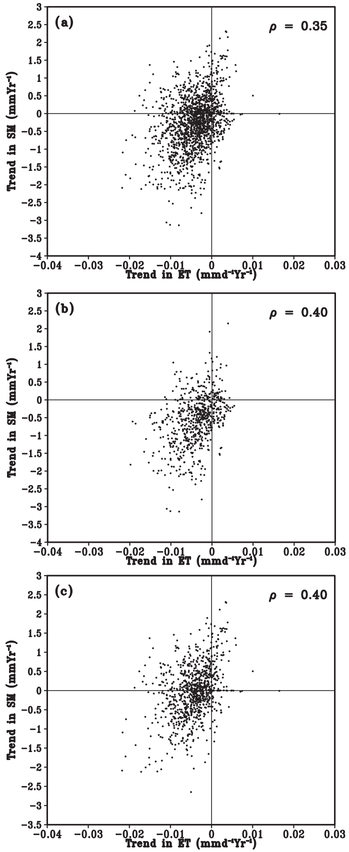

Figure 7. Scatter plot for trends in JJAS mean evapotranspiration (ET) vs. total soil moisture (SM) over the region 70–90° E; 10–28° N for the 55 year (1951–2005) period **(a)** for all the grid points; **(b)** for grid points with increasing trend and **(c)** for the grid points with decreasing trend in short wave radiation reaching at surface.

ESDD
6, 943–977, 2015

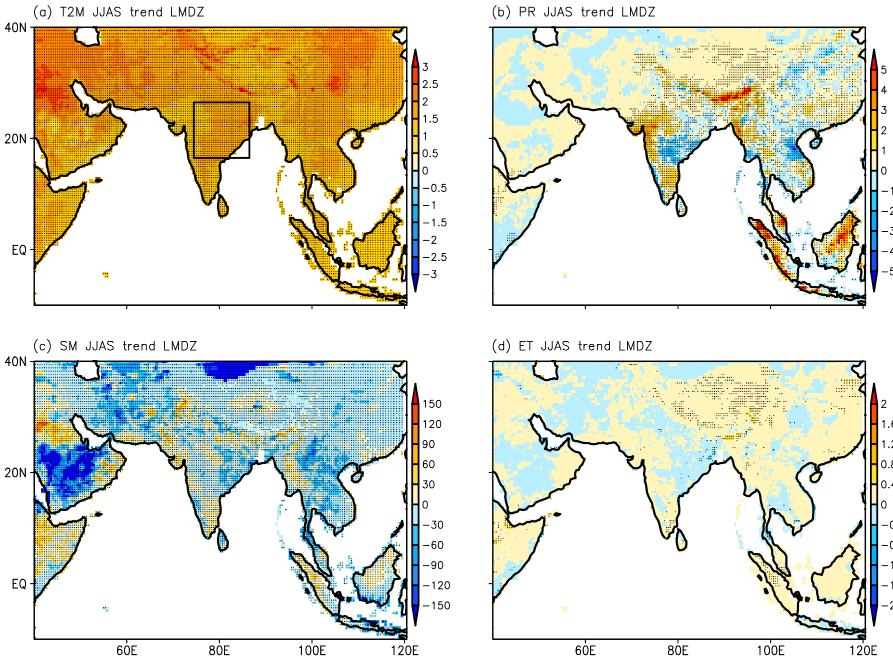

Figure 8. Spatial distribution of linear trends in **(a)** 2 m air temperature (°C), **(b)** precipitation (mm d^{-1}), **(c)** soil moisture (mm) and **(d)** evapotranspiration (mm d^{-1}) from RCP simulation of LMDZ. Trends are expressed as change over the period 2006–2095. Trend values exceeding the 95 % level of statistical significance based on Students *t* test are stippled. The box indicates central India (74.5–86.5° E; 16.5–26.5° N) region.

ESDD
6, 943–977, 2015

Understanding land surface response to changing South Asian monsoon in a warming climate

M. V. S. Ramarao et al.

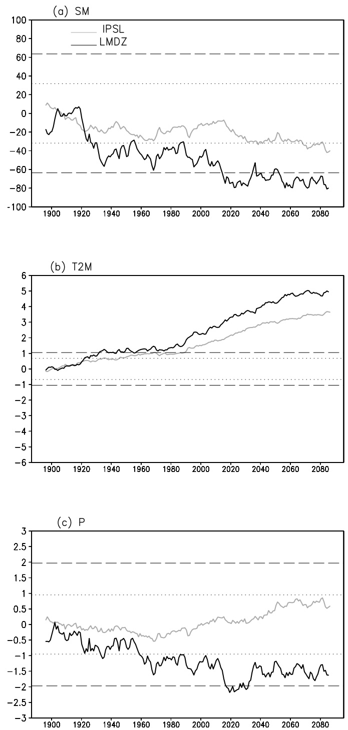

Figure 9. Time series of area-averaged anomalies of **(a)** soil moisture (SM; mm), **(b)** 2 m air temperature (T2M; °C) and **(c)** precipitation (P; mm d^{-1}) from ALL (HIST and RCP) experiments of (grey) IPSL and (black) LMDZ for the region 70–90° E; 10–28° N. The yearly JJAS anomalies are computed as the difference from the corresponding long-term mean (1886–2005) of NAT integration. Each time series has been smoothed by a 20 year running mean. The two horizontal dashed lines denote one SD limits from the NAT integration computed from the yearly JJAS averages for LMDZ and dotted lines correspond to IPSL.

ESDD
6, 943–977, 2015

Understanding land surface response to changing South Asian monsoon in a warming climate

M. V. S. Ramarao et al.